Signal-to-noise ratio analysis to estimate ocean wave heights from X-band marine radar image time series

J.C. Nieto-Borge, K. Hessner, P. Jarabo-Amores and D. de la Mata-Moya

Abstract: This work analyses the structure of the different contributions to the image spectrum derived by the three-dimensional Fourier decomposition of sea clutter time series measured by ordinary X-band marine radars. The goal of this investigation is to derive a method to estimate the significant wave height of the ocean wave fields imaged by the radar. The proposed method is an extension of a technique developed for the analysis of ocean wave fields by using synthetic aperture radar systems. The basic idea behind this method is that the significant wave height is linearly dependent on the square root of the signal-to-noise ratio, where the signal is assumed as the radar analysis estimation of the wave spectral energy and the noise is computed as the energy due to the sea surface roughness, which is closely related to the speckle of the radar image. The proposed method to estimate wave heights is validated using data sets of sea clutter images measured by a marine radar and significant wave heights derived from measurements taken by a buoy used as reference sensor.

1 Introduction

Ordinary X-band marine radars scan the water surface at grazing incidence with HH polarisation. These devices are suitable to be used as an active microwave remote sensing system for oceanographic purposes. The measurement of ocean waves with marine radars is based on the spatial and temporal structure analysis of the sea surface radar images. These radar images are due to the interaction of the electromagnetic waves with the sea surface ripples caused by the local wind [1–4]. This interaction produces a backscatter of the electromagnetic fields and therefore an image pattern in the radar display unit. This image pattern is commonly known by sailors as sea clutter, and it is considered as noise for navigation purposes. Using temporal sequences of consecutive sea clutter images, the spatial and temporal variability of the sea surface is analysed to extract an estimation of the directional wave spectrum [5–7], as well as related sea state parameters [8]. Because sea clutter values are related to the electromagnetic backscatter on the sea surface rather than the wave elevation, the directional wave spectrum estimated from the marine radar analysis is not properly scaled and therefore wave height values of the sea surface cannot be directly obtained.

This work investigates the structure of the sea clutter spectrum in order to propose a method to estimate the significant wave heights from the wave fields imaged by the radar. The method is an extension of a technique developed for ocean wave analysis by using spaceborne synthetic aperture radar (SAR) systems. The main idea behind is that the significant wave height is linearly dependent on the square root of the signal-to-noise ratio (SNR), where the signal is assumed as the total energy of the wave spectrum estimation derived by the sea clutter analysis mentioned above and the noise is computed as the energy due to the speckle caused by the sea surface roughness.

The paper is structured as follows. Section 2 introduces the basic ideas of the wave measurement technique by using marine radars. Section 3 takes into account the extension of the theory proposed for SAR systems, extending the analysis to those contributions to the image spectrum (e.g. the power spectral density of a sea clutter time series) that lead the wave height estimation of the wave field imaged by the marine radar. The structure of these spectral contributions to the image spectrum is investigated in Section 3 in order to derive a suitable definition of SNR ratio for marine radar, which permits to obtain reliable values of significant waveheights from sea clutter time series. Furthermore, once the structure of the mentioned spectral contributions to the image spectrum is analysed, Section 4 describes the proposed method to estimate ocean wave heights from marine radar sea clutter time series. This proposed method to estimate significant wave height is validated in Section 5 using comparisons between the radar results and in situ data. Finally, the conclusions of this investigation are summarised in Section 6.

2 Basics of the wave measurement theory by using X-band marine radars

The measurement of sea states using marine radars is based on backscatter of the electromagnetic waves by the ripples and the roughness of the free sea surface due to the local wind [3]. The pattern of electromagnetic energy backscattered by the ripples is modulated by the larger ocean surface structures, such as swell and wind sea waves, and therefore can be detected on the radar screen. Fig. 1 shows an example of sea clutter image taken by a

doi:10.1049/iet-rsn:20070027

Paper first received 22nd February and in revised form 14th May 2007

J.C. Nieto-Borge, P. Jarabo-Amores and D. de la Mata-Moya are with the Department of Signal Theory and Communications, Universidad de Alcalá, Spain

K. Hessner is with OceanWaveS GmbH, Lüneburg, Germany

E-mail: josecarlos.nieto@.uah.es

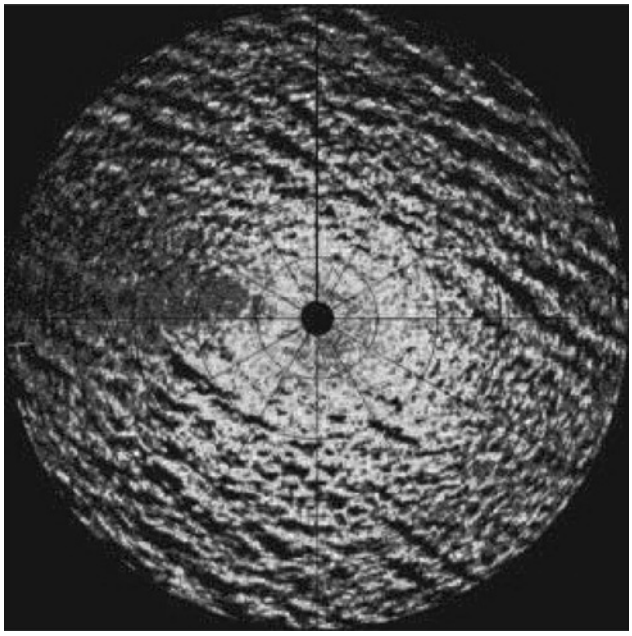

Fig. 1 *Digitised sea clutter image showing the backscatter phenomenon due to an ocean wave field*

marine radar on board a moving vessel in the North Sea. Different phenomena appear in the marine radar imaging:

- Range dependence [1].
- Azimuthal dependence with the wind direction [3].
- Wind speed dependence [3].
- Azimuthal dependence with the wave propagation direction [2, 3].
- Wave tilt modulation [3, 4].
- Shadowing modulation, which occurs when higher waves hide lower waves to the radar antenna [1, 4].
- Wave hydrodynamic and orbital modulation due to the motion of the water particles [9].

Analysing sea clutter data sets it can be realised that all these phenomena contribute with additional spectral components to the image spectrum, which do not belong to the wave field imaged by the radar [1–3]. All these phenomena have to be taken into account to analyse ocean waves from sea clutter time series. In addition, an appropriate ocean wave theoretical description has to be considered to extract useful information from the sea clutter. Therefore, the standard stochastic wave theory is taken into account [4]. This theory is briefly addressed in Section 2.1.

2.1 Stochastic description of sea states

Ocean waves are oscillations of the sea surface generated by the wind strength. Those waves present typical periods between 1 and 20 s (frequencies f beetwen 1 and 0.05 Hz) and wavelengths between 1 and 600 m. The wave elevation η for a specific position $\boldsymbol{r} = (x, y)$ at time t is usually described through the concept of sea state [10]. Sea states are wave fields with invariant statistical homogeneity in the spatial dependence and stationary in their temporal evolution. Under these assumptions, the free surface elevation $\eta(\boldsymbol{r}, t)$ has the following spectral representation [10]

$$\eta(\boldsymbol{r}, t) = \int_{\Omega_{k,\omega}} \mathrm{e}^{i(\boldsymbol{k}\cdot\boldsymbol{r}-\omega t)}\, \mathrm{d}Z(\boldsymbol{k}, \omega) + \text{c.c.} \qquad (1)$$

where 'c.c.' stands for complex conjugate, $\boldsymbol{k} = (k_x, k_y)$ is the two-dimensional wave number vector and $\omega = 2\pi f$ is the angular frequency of the ocean wave field. The integration domain $\Omega_{\boldsymbol{k},\omega}$ is defined as: $\Omega_{\boldsymbol{k},\omega} \equiv [-k_{x_c}, k_{x_c}) \times [-k_{y_c}, k_{y_c}) \times [0, \omega_c)$, k_{x_c}, k_{y_c} and ω_c being each spectral variable limit where ocean waves can be considered. In practical cases, k_{x_c}, k_{y_c} and ω_c are limited by the spatial and temporal sampling resolutions of the measuring sensor. The spectral random measures $dZ(\boldsymbol{k}, \omega)$ are complex amplitudes that are usually assumed as circular Gaussian random variables, statistically uncorrelated for different wave components $(\boldsymbol{k}, \omega)$. Under these assumptions, the sea surface elevation η can be regarded as a linear, homogeneous and stationary zero-mean stochastic process. The stochastic process defined by (1) is usually described by the so-called three-dimensional wave spectrum

$$F^{(3)}(\boldsymbol{k}, \omega) d^2k\, \mathrm{d}\omega = \mathcal{E}[\mathrm{d}Z(\boldsymbol{k}, \omega)\, \mathrm{d}Z^*(\boldsymbol{k}, \omega)] \qquad (2)$$

where $\mathcal{E}$ is the expectation operator, the asterisk indicates the complex conjugate and the upper index (3) denotes the dimension of the spectral domain where the spectrum is defined. It is well known that ocean waves are dispersive. Hence, there is a dependence between $\boldsymbol{k}$ and ω. For linear ocean, waves the dispersion relation is given by [10]

$$\omega = \varpi(\boldsymbol{k}) = \sqrt{gk \tanh(kd)} + \boldsymbol{k} \cdot \boldsymbol{U} \qquad (3)$$

where d is the water depth, $k = |\boldsymbol{k}|$ and $\boldsymbol{U} = (U_x, U_y)$ is the surface ocean current, or the relative speed between the wave field and the observer (e.g. in our case, the radar platform). The term $\boldsymbol{k} \cdot \boldsymbol{U}$ causes a Doppler shift in frequency. For linear ocean waves, only those wave spectral $(\boldsymbol{k}, \omega)$-components within the spectral domain $\Omega_{\boldsymbol{k},\omega}$ that hold the dispersion relation (3) are possible.

2.2 Description of the measuring technique

The procedure to analyse wave fields using a marine radar consists of measuring time series of N_t consecutive sea clutter images. The sampling time Δt of this temporal sequence of images corresponds to the antenna rotation period. The spatial resolutions (Δx and Δy) of each image depends on the azimuthal and the range resolution of the radar system.

To measure and store the radar data sets, an A/D converter (WaMoS II) built up for this specific purpose is used [3, 8]. WaMoS II is an operational Wave Monitoring System that was originally developed at the German GKSS Research Center Geesthacht. The measuring system consists of a conventional navigation radar, a high-speed video digitising and storage device and a standard computer (see the scheme shown in Fig. 2). The analogue radar video signal is read out and digitised into 256 grey levels. This information is transferred and stored on a computer where the wave analysis software carries out the computation of the sea state parameters in real time. For WaMoS II measurements, radar raw data are used. Hence, preprocessing filters (e.g. rain filter, anti clutter filter, image intensity amplification, etc.) are not applied.

Although WaMoS II system can be used for different kind of radars, the results presented in this work have been obtained using ordinary marine X-band radars, which work on HH polarisation, having an incoherent logarithmic amplifier and no frequency agility. The minimum requirements to use these kind of radars for ocean wave analysis are shown in Table 1 [4].

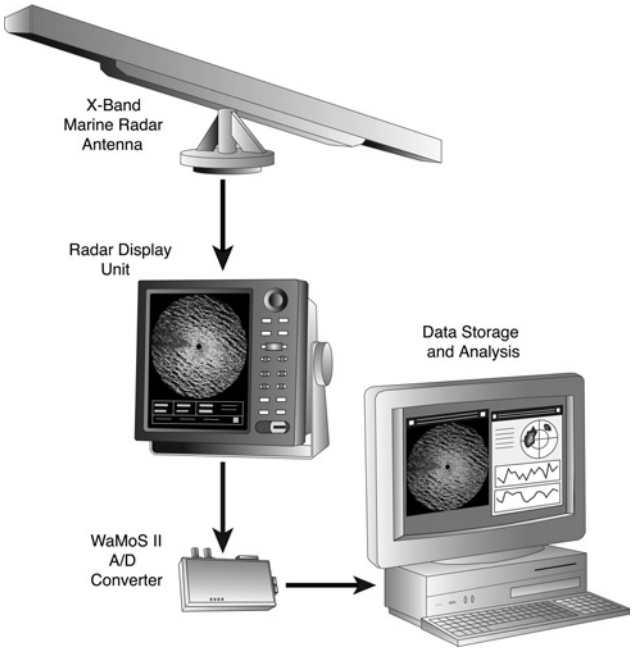

Fig. 2 *Scheme of an installation used for ocean wave measurement*

2.3 Analysis of temporal sequences of marine radar images

The estimation of the wave spectrum is carried out applying an inverse modelling technique to the digitised sea clutter image time series provided by the WaMoS II system [1, 4, 8]. Hence, the digitised data are transformed into the spectral domain by means of a three-dimensional discrete Fourier transform to estimate the so-called image spectrum $F_{\mathrm{I}}^{(3)}(\boldsymbol{k}, \omega)$ [1, 3]. From the image spectrum $F_{\mathrm{I}}^{(3)}(\boldsymbol{k}, \omega)$, first the surface current $\boldsymbol{U}$ is estimated by means of a least square fit using the dispersion relation (3) [3, 6, 7]. The dispersion relation, including the current contribution to the Doppler shift in frequency, is used to filter those $(\boldsymbol{k}, \omega)$ components of the image spectrum $F_{\mathrm{I}}^{(3)}$ which do not belong to the wave field [5, 6]. This filtered three-dimensional spectral estimation is denoted in this work as $F_{\mathrm{F}}^{(3)}(\boldsymbol{k}, \omega)$. Comparing the shape of this spectrum with the spectral estimations derived from insitu sensors, a further correction is needed [5]. This correction is derived empirically having the form of a wave number dependent transfer function $\mathcal{T}_{\mathcal{M}}(\boldsymbol{k})$ [1], which is multiplied to the filtered spectrum $F_{\mathrm{F}}^{(3)}$ to obtain an estimation of the three-dimensional wave spectrum $F_{\mathrm{W}}^{(3)}$ given by

$$F_{\mathrm{W}}^{(3)}(\boldsymbol{k}, \omega) = F_{\mathrm{F}}^{(3)}(\boldsymbol{k}, \omega) \cdot \mathcal{T}_{\mathcal{M}}(\boldsymbol{k}) \tag{4}$$

The function $\mathcal{T}_{\mathcal{M}}$ is known as modulation transfer function [4, 11]. It affects the variation of the filtered spectrum $F_{\mathrm{F}}^{(3)}$ along the dispersion relation line [1, 3].

Table 1: Marine X-band radar requirements for wave measurement

Parameter	Minimum value	Improvement
antenna rotation speed	32 rpm	faster
pulse length	80 ns	shorter
antenna length	2.5 m	longer
azimuthal resolution	0.8°	narrower

Note that the spectrum $F_{\mathrm{W}}^{(3)}$ given by (4) is not directly referred to the wave elevation η in the same way as the spectrum $F^{(3)}$ given by (2). This fact is due to the image spectrum $F_{\mathrm{I}}^{(3)}$ derived from grey-level values resulting in the WaMoS II digitalisation rather than wave elevation data. Thus, the values of these grey-levels depend on many factors: the backscatter of the electromagnetic fields due to the sea surface roughness, the marine radar features and set-up for each specific installation, the dynamical range of the WaMoS II digitalisation, etc. Hence, the grey-level values do not depend directly on how high the imaged waves are.

An example of an image spectrum $F_{\mathrm{I}}^{(3)}$ can be seen in Fig. 3. The figure shows a two-dimensional cut in the spectral domain $\Omega_{\boldsymbol{k},\omega}$ along the mean wave propagation direction. This spectrum has been obtained from a sea clutter time series measured by a radar station on shore located at the Northern coast of Spain (Bay of Biscay). Fig. 3 shows some of the main contributions to the image spectrum, such as the wave components, which can be identified by two branches of the dispersion relation (3), the first harmonic of the dispersion relation due to nonlinear mechanisms in the marine radar imagery [3, 4] and the background noise spectral components (BGN) due to the roughness of the sea surface [3, 4]. The existence of the BGN contribution to the image spectrum provides additional information to the sea surface imaged by the marine radar, which is not taken into account in the inversion modelling technique mentioned above. Section 3 deals with the investigation of the structure of the BGN spectrum in the three-dimensional domain $\Omega_{\boldsymbol{k},\omega}$.

3 Analysis of the three-dimensional spectral density of the background noise

As it was mentioned in the previous section, the analysis of the BGN spectrum due to speckle can inform about additional properties of the sea clutter that cannot be obtained from the assumptions considered for the inversion modelling technique described above. Therefore this spectral contribution to $F_{\mathrm{I}}^{(3)}$ has to be investigated. Hence, this

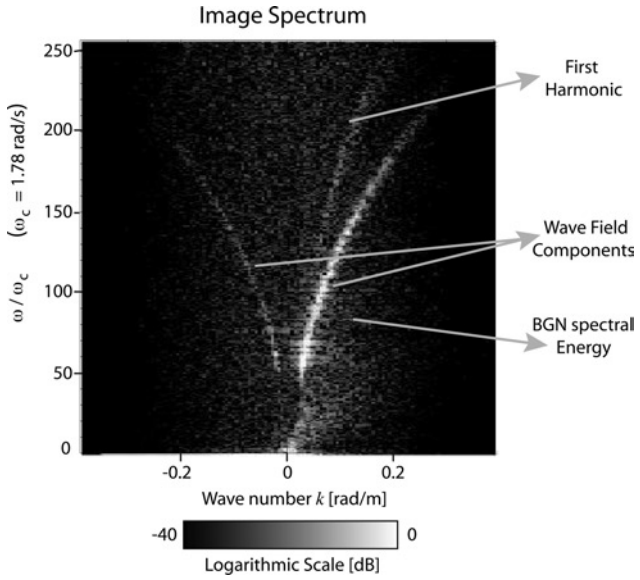

Fig. 3 *Example of a two-dimensional image spectrum where the main contributions can be identified*

Two different branches of the dispersion relation can be observed, the one with higher intensity corresponds to the waves approaching to the coast line, meanwhile the lower intensity dispersion relation branch is due to waves reflected by the coast

section addresses the study of the distribution of the BGN spectral components in the three-dimensional image spectrum $F_{\mathrm{I}}^{(3)}$. As it was mentioned above, the BGN spectral components are related to the sea surface roughness, which is responsible for the speckle noise in the marine radar images. Therefore the BGN spectral energy is closely related to all the meteorological and hydrodynamic phenomena that affect the sea surface on those spatial scales that are comparable to the electromagnetic wavelength (range of centimetres). As it can be seen in Fig. 3, the BGN spectral components are distributed almost along all the domain $\Omega_{\boldsymbol{k},\omega}$. In opposition, the wave components and the higher harmonics are clearly identified in $\Omega_{\boldsymbol{k},\omega}$ because their spectral components are located close to their respective dispersion relations [3, 4]

$$\omega_q = (q+1)\sqrt{\frac{gk}{q+1}\tanh\left(\frac{kd}{q+1}\right)} + \boldsymbol{k}\cdot\mathbf{U} \qquad (5)$$

where $q = 1, 2, \ldots$ is the order of the qth-harmonic. In practice, only the first harmonic (q = 1) has significant energy to be identified within the image spectrum domain (Fig. 3). Note that (5) is the dispersion relation of linear ocean waves (3) when $q = 0$.

Assuming that the speckle noise is a stochastic process statistically independent of the wave field contributions to the sea surface radar imagery (e.g. the wave and high harmonics spectral components), the BGN three-dimensional spectral density $F_{\mathrm{BGN}}^{(3)}(\boldsymbol{k}, \omega)$ can be expressed as a function of the image spectrum $F_{\mathrm{I}}^{(3)}(\boldsymbol{k}, \omega)$, the spectrum related to the wave components $F_{\mathrm{F}}^{(3)}(\boldsymbol{k}, \omega)$ and the high harmonic spectrum $F_{\mathrm{HH}}^{(3)}(\boldsymbol{k}, \omega)$, which is derived in a similar way to $F_{\mathrm{F}}^{(3)}(\boldsymbol{k}, \omega)$, but using the high harmonic dispersion relation given by (5). Therefore a BGN spectral density estimation can be obtained as

$$F_{\mathrm{BGN}}^{(3)}(\boldsymbol{k}, \omega) \simeq F_{\mathrm{I}}^{(3)}(\boldsymbol{k}, \omega) - F_{\mathrm{F}}^{(3)}(\boldsymbol{k}, \omega) - F_{\mathrm{HH}}^{(3)}(\boldsymbol{k}, \omega) \qquad (6)$$

It is important to address that (6) does not take into account all the spectral contributions to the image spectrum $F_{\mathrm{I}}^{(3)}$. Some of those image spectrum components that are not considered are the static patterns caused by the long range dependence on the sea clutter image [1], and the group line due to intermodulations between different wave field components [12]. These spectral contributions are located in a region of low frequencies [1, 13]. Hence, (6) is an approach for those frequencies higher than a given frequency threshold ω_{th}, which defines an appropriate limit between the ocean wave frequency domain and the low frequency region given by the static pattern and the group-line spectral components. This work uses $\omega_{\mathrm{th}} = 2\pi \cdot 0.04$ rad/s to define the frequency threshold. Hence, for those frequencies higher than ω_{th}, the static pattern cannot be considered and the group-line contribution to the total image spectrum energy is small compared with other image spectrum components [1, 13]. The spectral BGN domain $\Omega_{\mathrm{BGN}} \subset \Omega_{\boldsymbol{k},\omega}$, where (6) is taken into account, is defined as

$$\Omega_{\mathrm{BGN}} \equiv [-k_{x_c}, k_{x_c}) \times [-k_{y_c}, k_{y_c}) \times [\omega_{\mathrm{th}}, \omega_c) \qquad (7)$$

Furthermore, (6) assumes that, although the wave and the high harmonic components are not statistically independent, the location of these two components are separated enough in the spectral domain (Fig. 3) through their respectives dispersion relations given by (3) and (5). A more detailed discussion about the spectral energy distribution of the BGN spectrum $F_{\mathrm{BGN}}^{(3)}$ in the three-dimensional spectral domain $(\boldsymbol{k}, \omega)$ can be seen in following Section 3.1.

3.1 Structure of the BGN spectrum

Taking into account the limitations mentioned in the previous section, (6) permits us to estimate the BGN spectral density $F_{\mathrm{BGN}}^{(3)}(\boldsymbol{k}, \omega)$ for the spectral domain where the static patternsand the group-line components are not taken into account. For this spectral domain, the $(\boldsymbol{k}, \omega)$-distribution of the spectral components of $F_{\mathrm{BGN}}^{(3)}$ can be investigated. Hence, fixing constant values of the wave frequency ω, it can be seen that the $\boldsymbol{k}$ dependence of $F_{\mathrm{BGN}}^{(3)}$ is similar for different ω -planes (Fig. 3). This is due to the fact that speckle noise at a specific sea surface location is uncorrelated for different antenna rotations. This can be observed in Fig. 3, where the intensity of the BGN spectral components is independent of the frequency plane, depending only on the wave number $\boldsymbol{k}$. Hence, taking into account the statistical independence of $F_{\mathrm{BGN}}^{(3)}$ on the frequency, an averaged two-dimensional BGN spectrum $F_{\mathrm{BGN}}^{(2)}(\boldsymbol{k})$ due to the sea surface roughness can be estimated by integrating $F_{\mathrm{BGN}}^{(3)}(\boldsymbol{k}, \omega)$ along the ω -axis and dividing by the length of the frequency interval of integration

$$F_{\mathrm{BGN}}^{(2)}(\boldsymbol{k}) = \frac{1}{\omega_c - \omega_{\mathrm{th}}} \int_{\omega_{\mathrm{th}}}^{\omega_c} F_{\mathrm{BGN}}^{(3)}(\boldsymbol{k}, \omega)\, \mathrm{d}\omega \qquad (8)$$

Fig. 4 shows an example of two-dimensional BGN spectrum $F_{\mathrm{BGN}}^{(2)}(\boldsymbol{k})$ given by (8). It can be seen that $F_{\mathrm{BGN}}^{(2)}(\boldsymbol{k})$ presents higher values for lower wave numbers decaying as the wave numbers are increasing. This behaviour of the wave number dependence can be easily seen by integrating the two-dimensional BGN spectrum $F_{\mathrm{BGN}}^{(2)}(\boldsymbol{k})$ over all the wave number directions $\theta = \tan^{-1}(k_y/k_x)$

$$F_{\mathrm{BGN}}^{(1)}(k) = \int_0^{2\pi} F_{\mathrm{BGN}}^{(2)}(\boldsymbol{k}(k,\theta))k\, \mathrm{d}\theta \qquad (9)$$

where the multiplicative factor k inside the integral is the

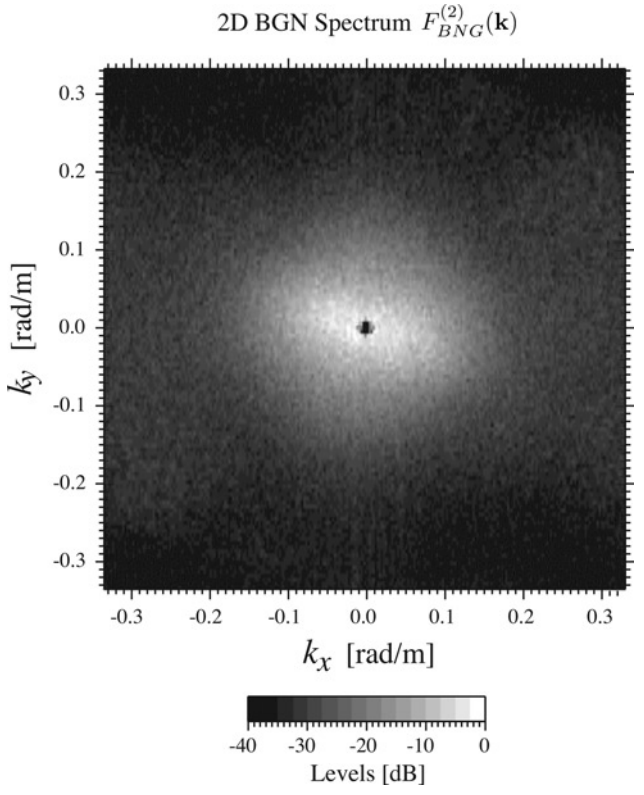

Fig. 4 *Two-dimensional speckle BGN spectrum* $F_{BGN}^{(2)}$ ***(k)*** *depending on the wave number* $\boldsymbol{k} = (k_x, k_y)$

Jacobian needed to change the Cartesian coordinates (k_x, k_y) to the polar coordinates (k, θ) used here to integrate along all the wave number directions θ. Fig. 5 shows the function $F^{(1)}_{\mathrm{BGN}}(k)/k$ resulting of applying (9) to the example shown in Fig. 4. The division by k is applied to avoid the Jacobian contribution to $F^{(1)}_{\mathrm{BGN}}(k)$. Furthermore, it can be seen that the normalised spectral density shown in Fig. 5 presents a constant value for high wave numbers ($k > 0.23$ rad/m). Following similar results derived from the sea surface detection using spaceborne SAR systems [9], this constant value of the BGN spectrum can be identified as the thermal noise of the sensor system.

In a similar way that the different wave number BGN spectra are obtained, the one-dimensional frequency BGN spectrum can be computed by integrating $F^{(3)}_{\mathrm{BGN}}(\boldsymbol{k}, \omega)$ over all the two-dimensional $\boldsymbol{k}$-domain, $\Omega_{\boldsymbol{k}} \equiv [-k_{x_c}, k_{x_c}) \times [-k_{y_c}, k_{y_c})$. Hence, an averaged one-dimensional frequency BGN spectrum $S^{(1)}_{\mathrm{BGN}}(\omega)$ can be obtained from $F^{(3)}_{\mathrm{BGN}}(\boldsymbol{k}, \omega)$ as

$$S^{(1)}_{\mathrm{BGN}}(\omega) = \frac{1}{4\, k_{x_c} k_{y_c}} \int_{\Omega_{\boldsymbol{k}}} F^{(3)}_{\mathrm{BGN}}(\boldsymbol{k}, \omega) d^2 k, \quad \omega_{\mathrm{th}} < \omega \leq \omega_c \tag{10}$$

where the normalisation factor $4\, k_{x_c} k_{y_c}$ is the area of $\Omega_{\boldsymbol{k}}$. The condition $\omega > \omega_{\mathrm{th}}$ is used again to avoid the static patterns and the group-line components, where the approach for $F^{(3)}_{\mathrm{BGN}}(\boldsymbol{k}, \omega)$, given by (6), cannot be considered. Fig. 6 shows the resulting spectrum $S^{(1)}_{\mathrm{BGN}}(\omega)$. It can be seen that the spectral energy values for each frequency interval are almost constant, which is consistent with the fact mentioned above concerning that the speckle is temporally uncorrelated for different antenna rotation periods.

The existence of the BGN contribution due to speckle links the oceanographic information derived from the marine radar with other types of microwave-based sensors, such as SAR [9]. Hence, a estimation of the wave SNR in the image spectrum can provide sea surface wave height information, which is not possible to be obtained from the spectrum $F^{(3)}_{\mathrm{W}}(\boldsymbol{k}, \omega)$ given by (4). Therefore Section 4 takes that idea into account and deals with the estimation of wave heights through the computation of the SNR from image spectrum of the sea clutter.

4 Use of BGN spectral energy to estimate the significant wave height

Significant wave height H_s is a well-known parameter used by oceanographers and ocean engineers to characterise the wave height of a wave field. Assuming a Gaussian wave field, H_s

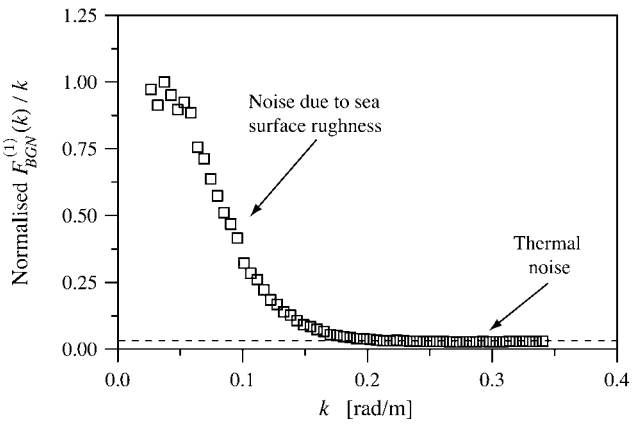

Fig. 5 *Normalised one-dimensional speckle BGN spectrum $F^{(2)}_{BGN}(K)/K$ depending on the wave number modulus $k=|\boldsymbol{k}|$*

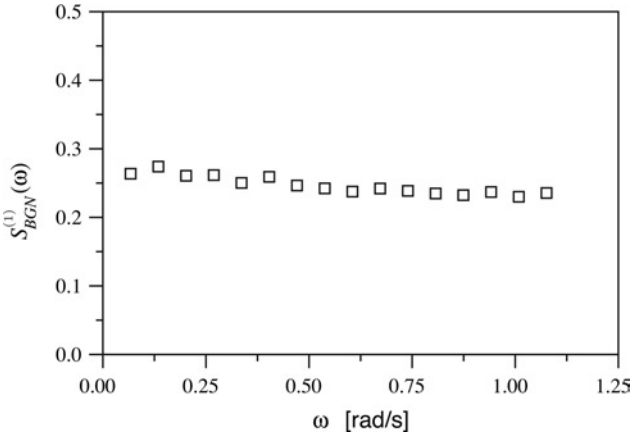

Fig. 6 *One-dimensional frequency BGN spectrum $S^{(1)}_{BGN}(\omega)$*

can be derived from the wave spectrum $F^{(3)}(k,\omega)$ [10] as

$$H_s = 4 \cdot \sqrt{\int_{\Omega_{k,\omega}} F^{(3)}(\boldsymbol{k}, \omega) d^2 k \; \mathrm{d}\omega} \tag{11}$$

As it was mentioned above, the ocean wave measurement with X-band marine radars has the particularity that the spectral densities $F^{(3)}_{\mathrm{W}}(\boldsymbol{k}, \omega)$ obtained after the inversion method described above contain information about values related to the scale of grey levels rather than values related to the wave elevation η. Thus, the non-scaled spectra $F^{(3)}_{\mathrm{W}}(\boldsymbol{k}, \omega)$ do not provide wave height estimations directly. Because of the existence of the background noise in the image spectrum of sea clutter, it is possible to extend the theory developed for two-dimensional wave spectrum estimation derived from spaceborne SAR imagery of ocean waves [9] to the three-dimensional case. Following this idea, the wave spectrum $F^{(3)}$ should be proportional to $F^{(3)}_{\mathrm{W}}$. Taking into account the theoretical results derived for two-dimensional wave number spectra derived from SAR imagery [9], the total energy defined by the three-dimensional wave spectrum $F^{(3)}$ should be proportional to the SNR in the sea clutter image, where the signal is assumed as the total energy of the image spectrum due to the wave spectral components and the noise is the total energy of the spectral noise caused by speckle. Hence

$$\int_{\Omega_{k,\omega}} F^{(3)}(\boldsymbol{k}, \omega) d^2 k \; \mathrm{d}\omega \simeq \mathrm{SNR} \tag{12}$$

Taking into account (11) and (12), a good estimation of the significant wave height H_s from sea clutter image time series must be proportional to the square root of SNR. Following this approach, H_s can be estimated by the following linear model

$$H_s = c_0 + c_1 \sqrt{\mathrm{SNR}} \tag{13}$$

where c_0 and c_1 are calibration constants, which are obtained empirically. The calibration constants c_0 and c_1 depend on each specific installation (e.g. platform height, angle of incidence, radar set-up, etc.) and SNR is the derived from the image spectrum. A proper definition of SNR must be consistent in the sense that no wave spectral components should be considered as speckle background noise components. On the other hand, any background noise contribution should not be considered as wave energy. The proposed definition of SNR takes into account the main features applied to the inversion modelling technique described above, as well as the energy of

the BGN spectrum. The following definition of SNR uses a non-scaled wave number spectrum $F_W^{(2)}(\boldsymbol{k})$ resulting in the frequency integration of the three-dimensional spectrum $F_W^{(3)}(\boldsymbol{k}, \omega)$ given by (4)

$$F_W^{(2)}(\boldsymbol{k}) = \int_{\omega_{th}}^{\omega_c} F_W^{(3)}(\boldsymbol{k}, \omega)\, d\omega \tag{14}$$

where ω_{th} is the same frequency threshold as the one used in (8). Therefore the proposed expression for SNR obtained for marine radar sea clutter time series is given by

$$\mathrm{SNR} = \frac{\int_{\Omega_k^\alpha} F_W^{(2)}(\boldsymbol{k}) d^2k}{\int_{\Omega_{BGN}} F_{BGN}^{(3)}(\boldsymbol{k}, \omega) d^2k\, d\omega} \tag{15}$$

where the integration domain Ω_{BGN} is given by (7) and Ω_k^α is defined as

$$\Omega_k^\alpha \equiv \left\{ \boldsymbol{k} \in \Omega_k \,\middle|\, F_W^{(2)}(\boldsymbol{k}) \geq \alpha \cdot \max\left[F^{(2)}\right]; 0 \leq \alpha \leq 1 \right\} \tag{16}$$

The parameter α is a threshold to avoid the contribution of the background noise within the dispersion shell filter.

5 Validation of the proposed relation between H_s and SNR using in situ data

To know if the proposed SNR definition given by (15) is a good approach to estimate the significant wave height H_s, it is necessary to carry out comparisons between H_s values derived from a reference measuring sensor and SNR estimations obtained from sea clutter images. Hence, and taking into account (13), if (15) is a good approach for SNR, the scatter plot of H_s measured by the reference sensor and the values of $\sqrt{SNR}$ derived from the radar analysis must be close to a straight line. To test the proposed method, a data set of in situ data recorded by a oceanographic buoy (e.g. the reference sensor) has been used. These buoy records are composed of sets of wave elevation time series. From the buoy data sets, the significant wave height values are derived computing the average of the one-third of the highest wave heights of the wave record. The data were acquired by the Floating Production and Storage Offshore (FPSO) Norne in the northern North Sea from November 1997 till January 1998. Fig. 7 shows the comparison between $\sqrt{SNR}$ computed from (15) using the marine radar data sets and values of H_s derived from the buoy records. It can be seen as a high value of the correlation coefficient (e.g. $r = 0.89$) with r.m.s. error equal to 0.38 m. Hence, the proposed linear model given by (13) fits quite properly with the obtained results. It should be pointed out that buoys measure wave properties in the temporal domain (e.g. wave elevation time series) at a fixed ocean location (e.g. the mooring point), whereas marine radar data are defined in both the spatial and the temporal domains. Hence, in contrast to buoy records, which provide a temporal average from the sea state parameters, marine radar measurements provide both spatial and temporal average of the sea state parameters derived from the wave spectral estimation.

In addition, it should be mentioned that the proposed method to estimate significant wave heights, which is inspired from a similar technique used at high grazing angles with space-based SAR images, has been applied for the specific case of the marine radar, where the sea clutter images are acquired under low grazing angle conditions. For high grazing angles, the original work applied

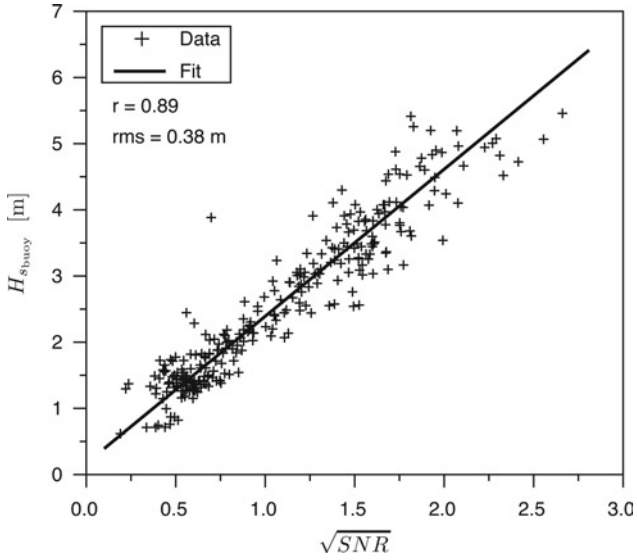

Fig. 7 *Scatter plot of marine radar $\sqrt{(SNR)}$ values versus significant wave height H_s measurements derived from oceanographic buoy records*

to spaceborne SAR images [9] was based on a fairly good understanding of electromagnetic backscattering from the sea surface. However, at low grazing angles, the electromagnetic scattering is still much less well understood, and it is necessary to take into account the additional phenomena such as breaking waves and diffuse scatter in order to derive a model to predict the average backscatter power [14]. Hence, it can be an informative result to know that a similar method for estimating significant wave height can work at low grazing angles as well.

6 Conclusions and outlook

This work investigates the structure of the background noise spectral density derived from the three-dimensional Fourier decomposition of sea clutter time series. This background spectral density is closely related to the sea clutter speckle caused by the sea surface roughness on short-spatial scales. The existence of this background spectral energy permits us to use ordinary X-band marine radars to extract ocean wave height information from sea clutter time series. The significant wave height H_s estimation is obtained analysing the SNR in a similar way to the methods proposed for SAR systems. For that purpose, an expression for the SNR has been proposed. The proposed expression for SNR considers the energy of the spectral components of the imaged wave field for the signal and the total spectral background energy of the three-dimensional image spectrum for the noise contribution to SNR. Using the in situ data, the proposed expression of SNR permits us to obtain a correlation coefficient of 0.89 between significant wave heights derived from the in situ data and the square root of SNR derived from radar measurements.

The background noise spectra contain more information than significant wave heights. This spectral contribution is closely related to the electromagnetic backscattering phenomena, which occur on the short spatial scale of the sea surface illuminated by the radar antenna. Hence, a parametrisation of this spectral density as a function of the wave number for given meteorological conditions and different radar features (e.g. angle of incidence, azimuthal and range resolutions, etc.) will be useful to increase the knowledge about the sea clutter structure and its behaviour at low grazing incidences.

7 Acknowledgments

This work has been supported by Universidad de Alcalá and Consejería de Educación de la Comunidad de Madrid (Spain), under Project CCG06-UAH/TIC-0726. In addition, the authors would like to thank Statoil ASA and the Spanish Port and Harbour Administration, Puertos del Estado, for the kind provision of the data.

8 References

1 Nieto-Borge, J.C., Rodríguez, G., Hessner, K., and Izquierdo, P.: 'Inversion of marine radar images for surface wave analysis', *J. Atmos. Ocean. Technol.*, 2004, **21**, (8), pp. 1291–1300

2 Dankert, H., and Rosenthal, W.: 'Ocean surface determination from X-band radar-image sequences', *J. Geophysical Res., Oceans*, 2004, **109**, C04016, doi:10.1029/2003JC002130

3 Ziemer, F., Brockmann, C., Vaughan, R.A., Seemann, J., and Senet, C.M.: 'Radar survey of near shore bathymetry within the OROMA project', EARSeL eProceedings, 2004, 3, (2), pp. 282–288

4 Nieto-Borge, J.C., and Hessner, K.: 'Comparison of WaMoS II with in situ measurements' in Hauser, D., Kahma, K., Krogstad, H.E., Lehner, S., Monbaliu, J.A.J., and Wyatt, L.R. (Eds.): 'Measuring and analysing the directional spectra of ocean waves EU COST Action 714, 2005, ISBN 92-898-0003-8, EUR 2136, p. 465

5 Ziemer, F., Rosenthal, W., and Carlson, H.: 'Measurements of directional wave spectra by ship radar'. IAPSO Symp., General Assembly, Int. Assoc. for Phys. Sci. of the OceansHamburg, Germany, 1983

6 Young, I.R., Rosenthal, W., and Ziemer, F.: 'A three-dimensional analysis of marine radar images for the determination of ocean wave directionality and surface currents', *J. Geophys. Res.*, 1985, **90**, (C1), pp. 1049–1060

7 Nieto-Borge, J.C., and Guedes, C.: 'Analysis of directional wave fields using X-band navigation radar', *Coastal Eng.*, 2000, **40**, (2000), pp. 375–391

8 Reichert, K., Hessner, K., Dannenberg, J., Tränkmann, I., and Lund, B.: 'X-band radar as a tool to determine spectral and single wave properties'. WAVES 2005 Proc., San Francisco, USA, 2005

9 Alpers, W., and Hasselmann, K.: 'Spectral signal to clutter and thermal noise properties of ocean wave imaging synthetic aperture radars', *Int. J. Remote. Sens.*, 1982, **3**, pp. 423–446

10 Komen, G.J., Cavaleri, L., and Donelan, M.: 'Dynamics and modelling of ocean waves' (Cambridge University Press, 2006)

11 Plant, W.J.: 'The modulation transfer function, concept and applications' in Komen, G.J. and Oost, W.A. (Eds.): 'Radar scattering from modulated wind waves' (Kluwer Academic Publishers, 1989), pp. 155–172

12 Frasier, S.J., and McIntosh, R.E.: 'Observed wavenumber-frequency properties of microwave backscatter from the ocean surface at near-grazing angles', *J. Geophys. Res.*, 1996, **101**, pp. 18391–18407

13 Stevens, C.L., Poulter, E.M., Smith, M.J., and McCregor, J.A.: 'Nonlinear features in wave-resolving microwave radar observations of ocean waves', *IEEE J. Ocean. Eng.*, 1999, **24**, (4), pp. 470–480

14 Saillard, M., and Sentenac, A.: 'Rigorous solutions for electromagnetic scattering from rough surfaces', *Waves Random Media*, 2001, **11**, R103–R137